Observations of debris and shrapnel plumes from PW driven solid targets

J. E. Andrew, R. D. Edwards, J. D. Fyrth, M. D. Gardner, A. J. Simons and K. Vaughan
Plasma Physics Department, AWE plc, Aldermaston, Reading RG7 4PR, UK

R. J. Clarke
Central Laser Facility, STFC, Rutherford Appleton Laboratory, HSIC, Didcot, Oxon OX11 0QX, UK

C. G. Allwork
Department of Physics, University of Surrey, Guildford GU2 7XH, UK

H. Doyle
The Blackett Laboratory, Imperial College, London SW7 2AZ, UK

Contact | **Jim.Andrew@awe.co.uk**

Introduction

During the course of the AWE experiments at Vulcan TAP in early 2008 glass witness plates were fielded to study debris and shrapnel plumes arising from a range of different solid targets. This work develops previous studies on long and short pulse debris studies performed by AWE[1,2,3,4]. The information will be used to reduce threats to optics and diagnostics that will be used in plasma physics experiments to be performed on the Orion laser facility[5,6] now being constructed at AWE.

Shrapnel and debris

In this report we will use the following definitions of shrapnel and debris. Debris is gaseous or liquid material target by-product that can produce a coating or feature on a surface without causing any physical damage to an optical surface or diagnostic component. These coatings may be absorbing or transmitting at the laser wavelength and may degrade an optical property (i.e. the transmission, reflection, scattering properties) or the laser damage threshold of an optical component. Shrapnel is a solid or liquid target by-product that can produce physical damage to an optical surface or component. Solid shrapnel causes permanent physical damage like craters or cracks in brittle materials and penetration holes in metal or polymer foils. Hot liquid droplets can cause thermally induced cracking, melting or physical damage in materials that they impact on. In addition to the material by-products from laser plasma targets, it is possible that radiation in the form of X-rays, neutrons, protons, electrons and electro-magnetic pulses may occur. These in turn could also interact with items inside the target chamber and themselves produce effects, e.g. radiation darkening of optical glass.

The targets and holders

Three types of targets were used that reflected the main aims of the experimental campaign. Tungsten targets of 4 mm and 1 mm thickness were utilised for X-ray production. Copper, Tantalum and plastic targets of 2 mm thickness were shot for γ-ray activation studies. Gold foils of 20 μm thickness were utilised for proton activation experiments. The 1 to 4 millimetre thick targets were mounted in a retaining target holder so that the target could be easily retrieved for post-shot inspection (figure 1).

The gold targets were mounted on simple aluminium posts and were always completely vaporised by the laser pulse. On two occasions the post was also hit by a part of the laser beam and this resulted in vaporisation of the tip of the aluminium post.

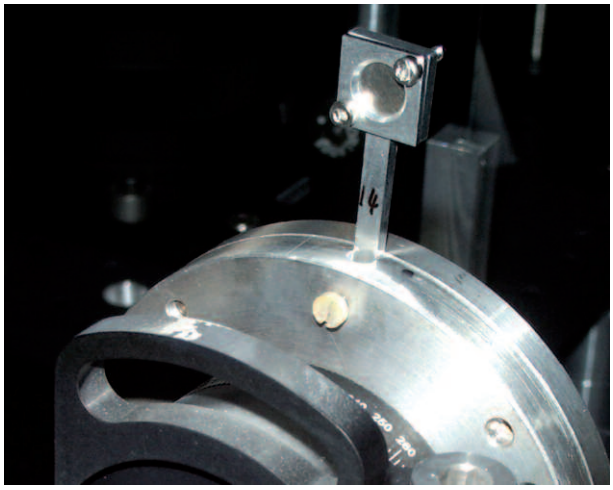

Figure 1. Retaining target holder with 1 mm thick Tungsten targets in place on the TAP target carousel. The body of the holder was made of aluminium and the two parts of the mount were held together with stainless steel bolts.

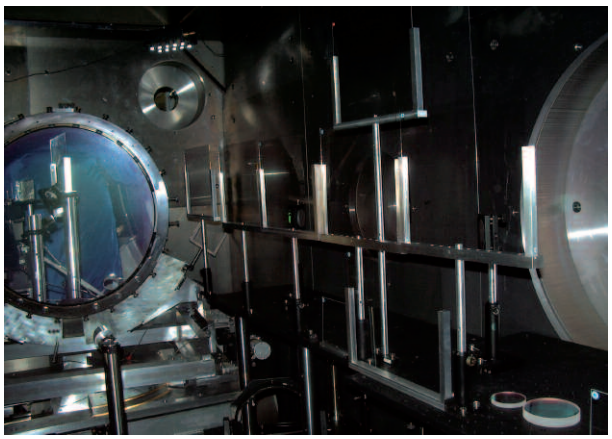

Figure 2. Focussing parabolic mirror (left) and array of glass witness plate holders (right) inside the TAP target chamber.

The experimental configurations

In order to catch any ejected target material, glass witness plates had to be arranged in the target chamber in such a manner so as not to be in the beam path but also allow material to be collected from both the front and rear faces of any targets. The plates also had to be out of any lines of sight required by the main experiment. Figure 2 shows an array of witness plate holders adjacent to the long wall of the target chamber and to the beam path from the final plane turning mirror and the off axis focussing parabola. The witness plates were either thin borosilicate glass (Schott D263T 253 mm × 205 mm × 0.55 mm) or soda lime glass (commercial float glass 253 mm × 205 mm × 2 mm). In addition a similar plate was placed behind the target to collect target material from the rear (unilluminated) surface of targets. For the gold foil targets a witness plate was also placed between the target, the incoming collimated laser beam and the incident focussing beam (figure 3). The closer proximity was necessary because the smaller mass of material needed to be collected at closer range over a smaller area in order to be visible.

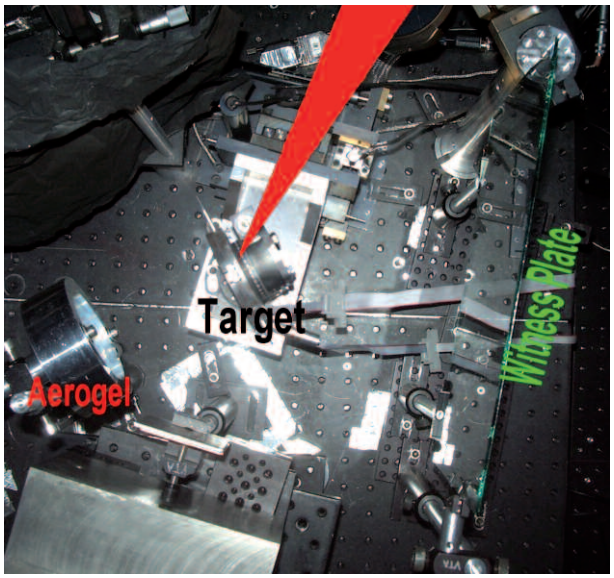

Figure 3. Close proximity witness plate used when firing thin gold foil targets. Target position is in the centre of the view. Laser beam is coming from the top right of view. An aerogel catcher was placed behind some targets to capture solid fragments.[3]

Post shot photography

The targets were examined after the experiments. In the case of the 1 mm Tungsten targets all had the centre of the target removed. A ring of material that had melted and then re-solidified often surrounded this central region. The rest of the target remained solid but with a number of cracks observed radiating from the point of laser material interaction towards the circumference of the target holder aperture (figure 4). Material from these targets was recovered on witness plates on both sides of the targets. Some of the target had also deposited back on to the target holder.

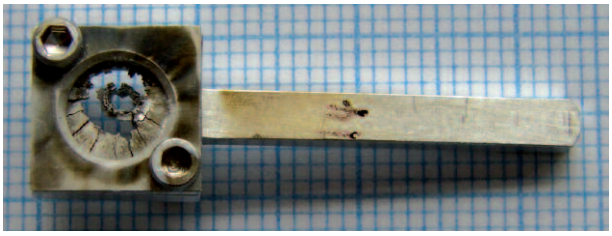

Figure 4. Post shot photograph of a 1 mm thick Tungsten target. Background grid is 1 mm squares.

The 4 mm thick Tungsten targets behaved differently. In this case a crater formed where the laser struck the target. Some radial cracking occurred but the target did not fragment like its thinner counterpart. For some examples the cracks were visible on the rear surface of the material but little or no debris and shrapnel was emitted from the rear of the target. Copious amounts of material were readily visible on witness plates placed to view the incident face emissions of the targets.

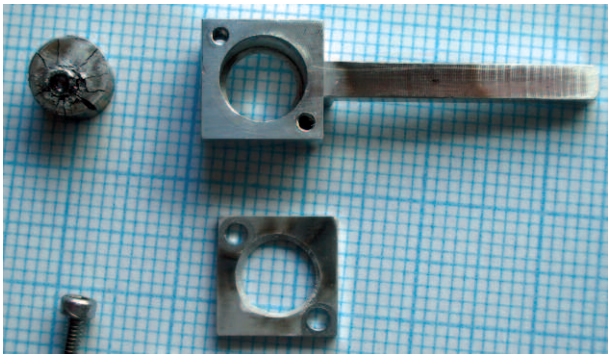

Figure 5. Post shot photograph of 4 mm thick Tungsten target and its holder. Background grid is defined by 1 mm squares.

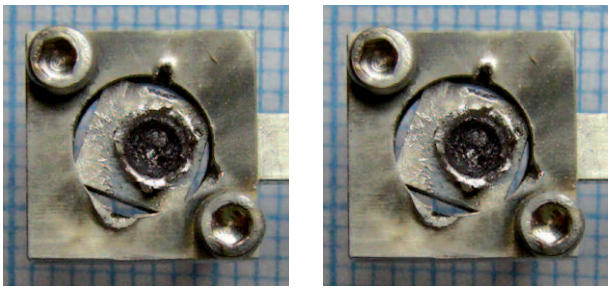

[a] [b]

Figure 6. Post shot photograph of a 2 mm thick Tantalum target and its holder. (a) Front surface (b) rear surface. Background grid is defined by 1 mm squares.

The 2 mm thick tantalum targets showed none of the cracking exhibited by the tungsten. At an incident on target energy of 330 J the front surface had a crater formed and at the rear surface material had spalled away. At lower energy (150 J) the input face still suffered cratering (figure 6a) and the rear face was deformed into a hump indicating that the material was on the verge of spalling (figure 6b). The copper target irradiated at 364 J also failed to remain intact on the rear surface in a similar manner to tantalum. The 2 mm thick plastic target looked visually as though it had been completely vaporised by a laser pulse of 390 J but later

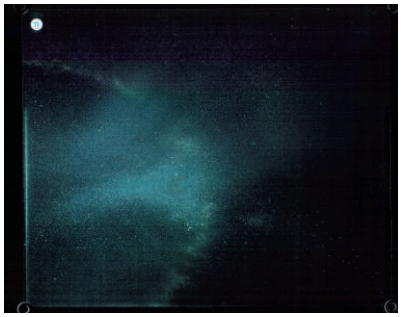

Figure 7. Glass witness plate #B73, position as in Figure 3. 4 mm thick W target. Target incident energy = 295 J. Shot #13_18-03-08. Incident face target emissions.

Figure 8. Glass witness plate #R79. 1 mm thick W target. Target incident energy = 311 J. Shot #07_05-03-08. Rear face target emissions. Single shot exposure.

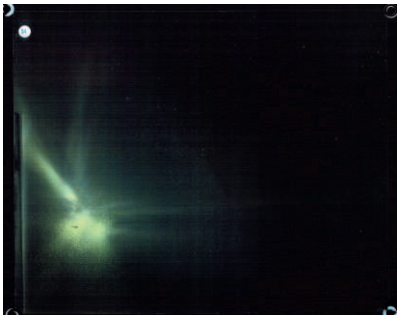

Figure 9. Glass witness plate #B84, position as in Figure 3. 20 µm thick Au target. Target incident energy = 341 J. Shot #01_20-03-08. Incident face target emissions. Single shot exposure.

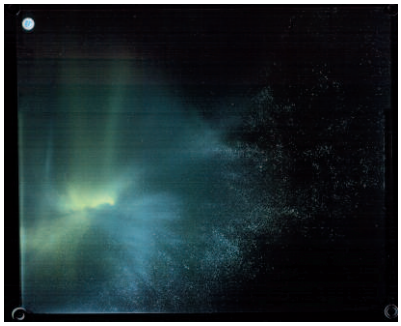

Figure 10. Glass witness plate #B87, position as in Figure 3. Two 20 µm thick Au targets. Double shot exposure. Target incident energies = 374 and 339 J. Incident face target emissions.

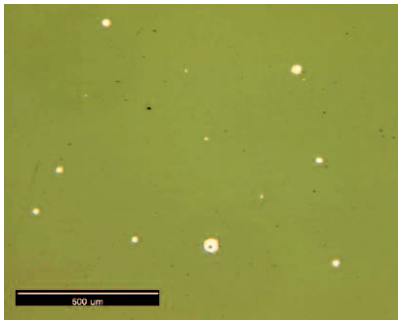

Figure 11. Reflected light micrograph of debris features. Scale bar = 500 µm. Glass witness plate #R79. 1 mm thick W target. Target incident energy = 311 J. Shot #07_05-03-08. Rear face target emissions.

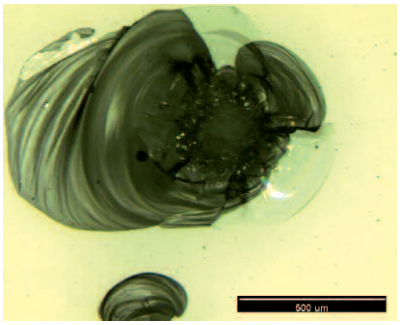

Figure 12. Reflected light micrograph of an impact crater caused by shrapnel. Scale bar = 500 µm. Glass witness plate #R79. 1 mm thick W target. Target incident energy = 311 J. Shot #07_05-03-08. Rear face target emissions. Single shot exposure.

inspection of a witness plate behind the target showed that modified material had been collected and some fragments had caused craters to be produced in the glass surface.

Witness plate evaluation

The post-shot surfaces of the witness plates were recorded by using flat bed scanning at a resolution of 600 dpi. Simple visual evaluation of the images for particulate, cratering and coating was used to prioritise the inspection of the 190 witness plates obtained during the course of the experimental campaign. Some examples of the witness plates are shown in figures 7-10 for various target conditions.

Figure 7 shows the material collected from the incident face of a 4 mm tungsten target irradiated with a 295 J laser pulse. The deposition consists of a thin ring of material extending over half of the plate. There is also another area extending from the centre of the ring outwards across 75% of the width of the plate.

Figure 8 illustrates a witness plate placed behind a 1 mm tungsten target showing a well-defined circle of impact craters (top left quadrant) with a diameter of ~140 mm.

Figure 9 shows the debris plume from a single 20 µm thick gold foil target irradiated by a 341 J pulse. The plume was not symmetric and has a number of ray features.

Figure 10 illustrates the material plumes from the incident face of two 20 µm thick gold targets with target incident energies of 374 and 339 J where the second pulse also irradiated the end of the aluminium mounting stalk (figure 13). The material from the foils occupies the left hand third of the image. The material from the vaporised end of the target stalk extends from the lower left corner of the witness plate to the centre of the right edge.

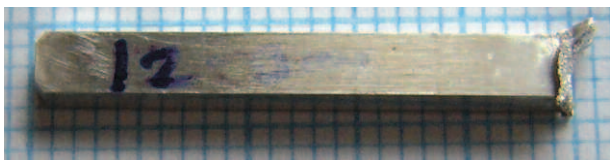

Figure 13. Aluminium stalk for mounting a 20 µm thick gold target after irradiation by part of the focussed beam. The material from the top millimetre of the stalk was vaporised and contributed to the debris plume shown in figure 10. Background grid is defined by 1 mm squares.

Witness plate microscopy

Although flat bed scanning was useful for rapid, preliminary evaluation of material plumes it was necessary to utilise microscopy to fully identify the nature of debris and shrapnel features on the surface of the witness plates.

Figures 11 and 12 show two different types of features. Figure 11 shows target material from a location in the top right quadrant of figure 8 where the flat bed scanned image showed little or no indication of any features. The light circular features can be identified as molten metal splats by using higher magnification inspection. In this case the features are circular because the impacts occur at small angles of incidence. For impacts at higher angles and grazing angles these circular features may spread into comet like features with a small bright feature sometimes surrounded by a halo of material and numerous narrow streaks of material spreading away from the point of impact (figure 14).

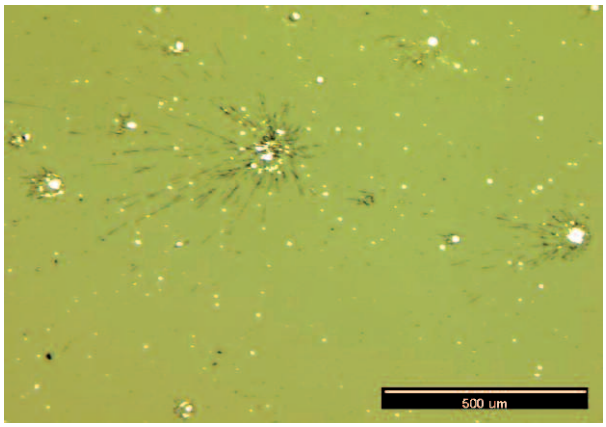

Figure 14. Molten metal impact features caused by high incidence angle impact of front face target material. Scale bar = 500 µm. Two 1 mm W targets, target energies = 311 and 315 J.

For higher kinetic energy impacts, the target material causes the formation of craters in the glass witness plates. The craters can be much larger than the incident particles because cracks propagate rapidly in glass. Figure 12 shows an impact crater from the central region of the shrapnel plume of figure 8. The darker parts of the image are surface or near surface damage of the material. The conchoidal fracturing and lighter features are damage propagating deeper into the glass.

Quantifying a shrapnel plume

Typically, micrographs consisted of multiple light and dark features on a medium, uniform background colour. The light features were usually metal particles and the dark features were often impact craters or sometimes flakes of low reflectivity metal foils. Where gold and copper targets were used it was easy to distinguish target material from mount material by the colours of the features observed on the witness plates. When the locations of micrographs were recorded it was possible to map the distribution of debris and shrapnel features across a plate. Figure 15 illustrates the distributions of the largest craters and metal debris for the witness plate shown in figure 8. Data from three horizontal scans (vertically separated by 5 mm) through the centre of the shrapnel plume recorded by the plate are shown.

The crater dimensions were generally one or two orders of magnitude larger than the metal debris spots. The larger craters (c.f. figure 12) require larger projectile kinetic energies and the distribution indicated that the higher energy target fragments were in the centre of the plume and that the envelope was approximately symmetric. Under the envelope there was also a distribution of lower energy fragments. The maximum size of metal debris spots (c.f. figure 11) varied between a few microns and 50 µm across the whole plate and extended beyond the region where shrapnel damage occurred.

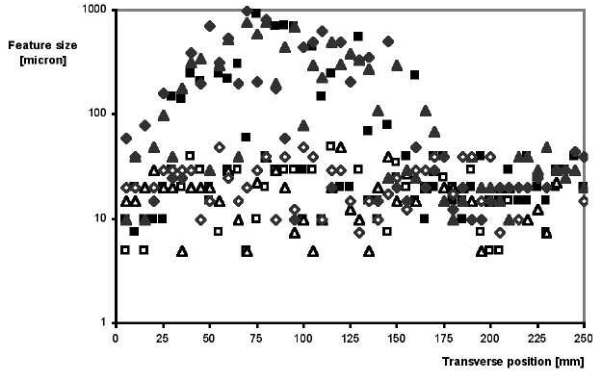

Figure 15. Quantitative micrograph analyses from figure 8. The horizontal axis is transverse position (x=0 corresponds to the left edge of the plate in figure 8, 215mm from the target). The vertical axis is feature size. The black symbols indicate the maximum crater dimension in a micrograph. The white symbols represent the maximum metal debris dimension. Square, triangle and diamond symbols indicate data from transverse scans taken at 150, 155 and 160 mm from the lower edge of the witness plate.

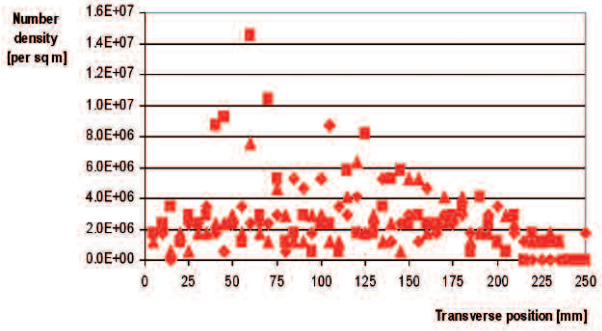

Figure 16. Quantitative micrograph analyses from figure 8. The horizontal axis is transverse position. The vertical axis is number density of metal debris. Square, triangle and diamond symbols indicate data from transverse scans taken at 150, 155 and 160 mm from the lower edge of the witness plate.

Figure 16 illustrates the number density distribution of molten metal spots. Across most of the plate the density varied in the range 1 to 6×10^6 m^2. Isolated occurrences of high numbers of small spots occurred near the centre of the shrapnel pattern where densities peaked at 14×10^6 m^2.

Activation

Post shot monitoring of some targets and witness plates recorded levels of activation that required temporary isolation of the items. Radioactive material from the

targets was observed by autoradiography to deposit back onto the target mount as well as on to witness plates. For close proximity witness plates the soda lime glass was preferred to the borosilicate as it was less affected by radioactive activation by proton beams. Figure 17 shows the decay of activation from a 1mm tungsten target and its mount. Later, separate autoradiographs indicated that most of the activity arose from the stainless steel bolts holding the two parts of the target mount together.

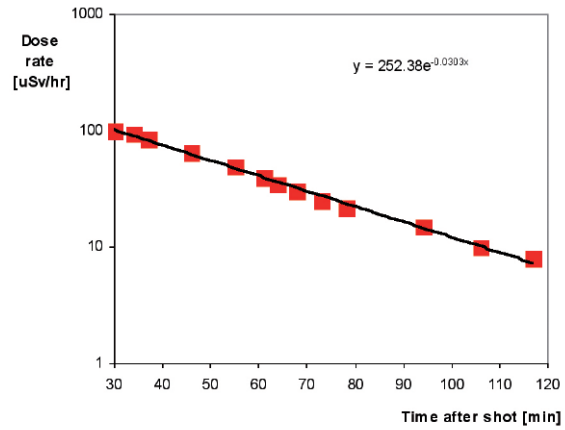

Figure 17. Dose rate measured by Geiger counter 10 mm from Tungsten target assembly as a function of time.

The measured half life derived from figure 17 was dominated by the decay of ^{52}Mn as a result of the ^{52}Cr(p,n)^{52}Mn reaction produced via proton activation of the chromium in the stainless steel.

Conclusions

This report only covers the data analysis performed in the three months following the experiment. The large number of witness plates and the form of the information to be recovered imply that many months will be required for a comprehensive analysis. The observations indicate that the debris and shrapnel plume characteristics depend strongly on the size, shape and thickness of the target, how it is mounted and the laser irradiation conditions. Improved image analysis software will need to be developed to automate the material distribution aspects of the work. The shrapnel and debris distributions can then be mapped on to the Orion target chamber to identify ports, diagnostic and optics that may be degraded or damaged by sustained target operations in the future.

Acknowledgements

We wish to acknowledge the support and assistance of the target fabrication groups at AWE and CLF for suggestions on target mounting, preparation and post shot inspection. We also wish to thank Dr Wigen Nazarov of St. Andrews University for the foams used on some of the tungsten targets.

References

1. J. C. Watson, J. E. Andrew and N. J. Bazin, *Investigation of high power laser beam, plasma, debris and shrapnel induced damage of optical coatings on the HELEN laser facility*. SPIE conference proceedings 76-87, vol. 4932 (2003).
2. J. E. Andrew, K. R. Mann, M. T. Tobin and J. C. Watson, *The influence of 527nm laser light on debris and shrapnel contaminated optical surfaces.* SPIE conference proceedings 147-157 vol. 4932 (2003).
3. M. Tobin, J. Andrew, D. Haupt, K. Mann, J. Poco, J. Satcher, D. Curran, R. Tokheim and D. Eder, *Using silica aerogel to characterize hypervelocity shrapnel produced in high power laser experiments.* Intnl. Jnl. of Impact Engineering, 713-721, **29**, (2003).
4. J. D. Griffiths and J. E. Andrew, *Characterisation of short pulse laser target debris at the HELEN laser facility.* SPIE conference proceedings 59910L-1, vol. 5991 (2005).
5. D. Landeg and C. Edwards, Project Orion, Plasma Physics Department, Annual Report p5, 2005, AWE plc
6. C. Edwards and E. Edwards, Introduction to the Orion Project, Plasma Physics Department, Annual Report p4, 2006, AWE plc